Time-Resolved Coherent Diffraction of Ultrafast Structural Dynamics in a Single Nanowire

Marcus C. Newton,[1,2,*] Mayu Sao,[3] Yuta Fujisawa,[3] Rena Onitsuka,[4,5] Tomoya Kawaguchi,[6] Kazuya Tokuda,[6] Takahiro Sato,[4] Tadashi Togashi,[7] Makina Yabashi,[4] Tetsuya Ishikawa,[4] Tetsu Ichitsubo,[6] Eiichiro Matsubara,[6] Yoshihito Tanaka,[4,5] and Yoshinori Nishino[3]

[1] *Research Institute for Electronic Science, Hokkaido University*
[2] *Department of Physics & Astronomy, University of Southampton, UK*
[3] *Research Institute for Electronic Science, Hokkaido University, Sapporo 001-0021, Japan*
[4] *RIKEN SPring-8 Center, RIKEN, 1-1-1, Kouto, Sayo, Hyogo 679-5148, Japan*
[5] *Department of Physics, School of Science and Technology, Kwansei Gakuin University, Gakuen, Sanda, Hyogo 669-1337, Japan*
[6] *Department of Materials Science and Engineering, Kyoto University, Kyoto 606-8501, Japan*
[7] *Japan Synchrotron Radiation Research Institute (JASRI), 1-1-1 Kouto, Sayo-cho, Sayo-gun, Hyogo 679-5198, Japan*

(Dated: April 11, 2014)

The continuing effort to utilise the unique properties present in a number of strongly correlated transition metal oxides for novel device applications has led to intense study of their transitional phase state behaviour. Here we report on time-resolved coherent X-ray diffraction measurements on a single vanadium dioxide nanocrystal undergoing a solid-solid phase transition, using the SACLA X-ray Free Electron Laser (XFEL) facility. We observe an ultra-fast transition from monoclinic to tetragonal crystal structure in a single vanadium dioxide nanocrystal. Our findings demonstrate that the structural change occurs in a number of distinct stages attributed to differing expansion modes of vanadium atom pairs.

Correlated electronic materials are those in which the electronic interactions are not readily predicted through a study of the individual constituents. These materials often undergo a phase transition when subject to excitation, where quantities including either electronic structure, crystal structure or magnetic ordering are significantly altered. This process is often driven by a change in temperature but may also occur due to electrical, mechanical, optical and magnetic excitations.[1–4]

Simple models of correlated systems have proven difficult to solve due to the large number of interactions that must be accounted for. As a result, accurately simulating theoretical predictions is often impractical and leaves little to guide experimental studies.[5] There remains therefore the challenge to develop a dynamical theory that is able to describe spontaneous atomic rearrangement due to external excitation. In addition, there are few studies dedicated to time resolved measurements. This is largely due to the limitations of the available tools for studying such systems. For example, electron microscopes are able to resolve atomic scale features of sufficiently thin materials but are in general limited to pico-second time resolution.[6] The key to deciphering these phenomena lies in measuring the time-dependent changes in atomic structure. Observation of the dynamical behaviour is permitted only when the time scale for measurement is appropriately less than that of the phase change phenomena.

Vanadium dioxide (VO_2) is a transition metal oxide material that exhibits a solid-solid phase transition from tetragonal to monoclinic atomic ordering at a critical temperature $T_c = 67.9°C$ which is accompanied by a metal-to-insulator phase transition. In the monoclinic (tetragonal) phase, VO_2 belongs to the $P2_1/c$ ($P4_2/mnm$) space group respectively. The structural change in VO_2 can occur on the femtosecond timescale, as demonstrated here. There is still however some debate on the nature of the transition due to conflicting results, with authors subscribing to either the Mott-Hubbard or Peierls dominated interactions.[7–10] A change in conductivity, several orders of magnitude in size, across T_c has made VO_2 a long standing topic of research with the aim of developing potential device applications where ultra-fast switching characteristics are desirable.[11–14]

The advent of 4$^{\text{th}}$ generation X-ray Free-Electron Laser (XFEL) facilities, as a tool for materials analysis, is proven to provide unprecedented insight into nanometre scale structure. [15–18] These studies demonstrate the potential that high brilliance light sources have for advancing our understanding of a wide range of phenomena. Coherent X-ray diffraction (CXD) imaging is a powerful lens-less imaging tool for probing materials with nanometer resolution.[19] Conventional CXD is performed by illuminating a sample with a spatially coherent X-ray source so that the coherence area exceeds the dimensions of the crystal; a condition that is always satisfied for an XFEL source, when the X-ray beam size is larger than the sample. In the Bragg reflection geometry, scattered light from the volume of the crystal interferes to produce a coherent diffraction pattern in the far-field.[20–22]

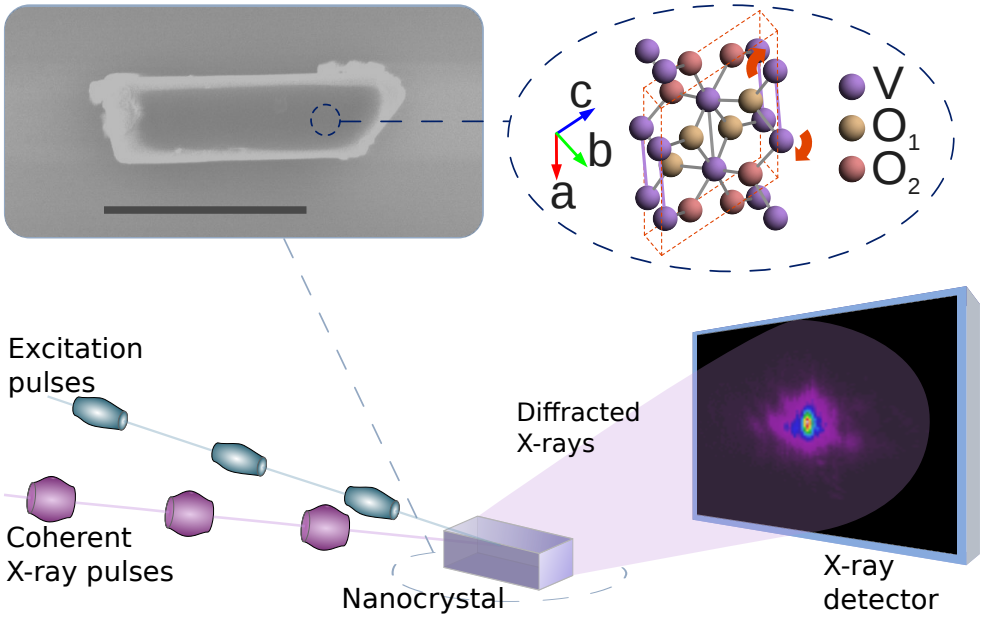

FIG. 1. **Schematic of the experiment**. The sample is mounted in the Bragg reflection geometry. At time t, the sample is excited with a femto-second pulse of light from the Ti:Sapphire laser. After a known time interval $\Delta t = t' - t$, the sample is probed with a femto-second pulse from the XFEL. By varying Δt, we were able to obtain coherent diffraction information on the time evolution of the process. The inset shows a scanning electron micrograph image of a single vanadium dioxide (VO_2) nanocrystal on the surface of a Si (100) substrate. A 1 micron scale bar is shown. Also shown inset is an illustration of the atomic arrangement in the VO_2 unit cell for the monoclinic (M_1) structure.

The diffracted intensity is measured using an area detector which is positioned far enough away from the sample to resolve the finest fringes of the coherent diffraction pattern. Iterative phase reconstruction methods are then used to recover the complex electron density $\rho(\mathbf{r})$ and phase information $\phi(\mathbf{r})$. This in turn provides information on the atomic displacements throughout the volume of the crystals according to the relation $\phi(\mathbf{r}) = \mathbf{Q} \cdot \mathbf{u}(\mathbf{r})$, where $\mathbf{u}$ is the atomic displacement.[23]

In the following we combine time resolved pump-probe measurements with coherent X-ray diffraction. This method is used to study structural changes in self-assembled vanadium dioxide nanocrystals. Time-resolved measurements were achieved using a pump-probe scheme consisting of a femto-second Ti:Sapphire laser system as an optical pump and the XFEL as a femto-second probe. The XFEL is particularly suited to the study of structural phase transitions in solid state materials due to its femto-second timing resolution and spatial coherence. Measurements were performed at the SPring-8 Angstrom Compact Free Electron Laser (SACLA) facility in Japan. SACLA is a compact XFEL operating down to $\sim$ 0.6 Å in wavelength. [24] Coherent diffraction experiments were performed in air on a single VO_2 nanocrystal in the Bragg reflection geometry. Pump-probe measurements were performed in the usual way. Namely, at time t, the sample was excited with a femto-second pulse of light from the Ti:Sapphire laser. After a known time interval $\Delta t = t' - t$, the sample was probed with a femto-second pulse from the XFEL. By varying Δt, it was possible to obtain coherent diffraction information on the time evolution of the process. By inverting the coherent diffraction pattern, a real-space image of the object can be obtained. Further details on data compilation can be found in the Supplementary Information.

Figure 1 illustrates the geometry of the experiment. The XFEL was operated with an unfocused beam size of 250 microns in diameter. The photon energy and duration was 8.682 keV and $\sim$10 femto-seconds respectively with a typical flux of 10^9 photons per pulse, after passing through a Si(111) double-crystal monochromator.[25] The Ti:Sapphire excitation laser was operated at a wavelength of 800 nanometers. A pulse energy of 300 micro Joules per pulse was achieved using a chirped pulse amplifier system. The full-width-half-maximum of the excitation beam was reduced to 460 microns in size before impinging on the sample. Both beams were caused to coincide at the sample surface with less than 100 microns accuracy. Position jitter was not a major concern when using the unfocussed XFEL beam for studying a single nanometre scale crystal as the crystal was significantly smaller than the beam and fully illuminated. Timing between the pump and probe lasers was controlled using an all optical system with the initial delay time tuned using

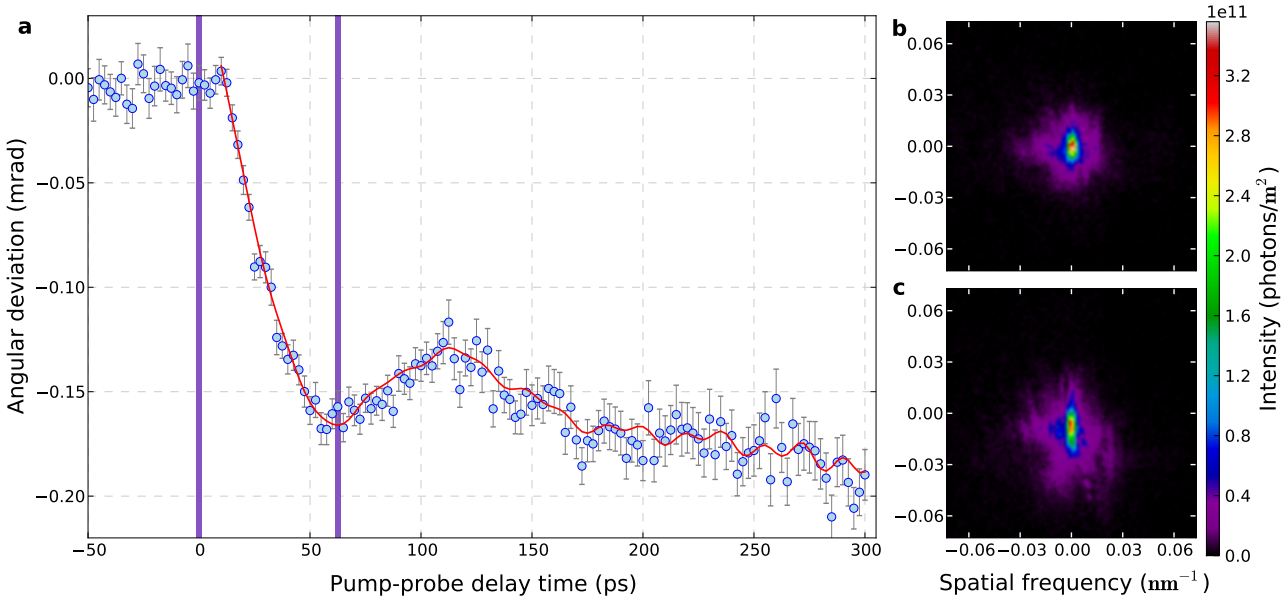

FIG. 2. **Time dependent angular deviation of the coherent diffraction pattern**. **a**, Deviation of the mean displacement of the coherent diffraction pattern in response to excitation at a fluence of 102 mJ/cm^2 per pulse from the Ti:Sapphire femto-second laser. **b**, Coherent diffraction pattern at delay time of 0 ps. **c**, Coherent diffraction pattern at delay time of 62.5 ps. Each diffraction pattern consists of the accumulation of data from 25 XFEL shots.

a fluorescent reference sample. The point zero time delay was calibrated down to an accuracy of $\sim$ 10 ps. The detector, XFEL and Ti:Sapphire laser were operated at 20 Hz, 10 Hz and 5 Hz respectively allowing interleaving of background data and unperturbed coherent diffraction data acquisition.

VO_2 nanocrystals were prepared using a chemical vapour deposition process. An isolated single VO_2 nanocrystal was then prepared so that the (011) reflection in the low temperature monoclinic phase is approximately specular (see Methods section). In the high temperature tetragonal phase, the (110) reflection is also approximately specular (see Supplementary Information). The sample was mounted on a custom built ceramic heated stage, designed by the authors, which was subsequently mounted onto a Kohzu (ϕ, χ, θ) goniometer. The propagated wave was largely concealed in a vacuum path chamber with Kapton polyimide windows at either end between the sample and detector. A multiport CCD X-ray detector was used to acquire coherent X-ray diffraction patterns. The detector was mounted at a distance of 1410 millimetres normal to the reflected wave and at an angle of 2θ, as illustrated in figure 1.

As the phase transition of VO_2 exhibits a well defined hysteresis between the thermodynamically stable low temperature monoclinic and high temperature tetragonal phases, the pump-probe experiment was performed below the hysteresis temperature. It was found that 30°C was a sufficient temperature to avoid hysteresis effects (see Methods section).

Figure 2**a** shows the angular deviation of the coherent diffraction pattern for varying delay times, in response to excitation at a fluence of 102 mJ/cm^2 per pulse from the Ti:Sapphire femto-second laser. Measurements were performed in the low temperature monoclinic Bragg geometry. Each data point results from the accumulation of data from 25 XFEL shots with dark-field subtraction, as described in the Supplementary Information. The delay interval between each data point was 2.5 pico-seconds. Immediately after time zero, a fast reduction in the Bragg angle was observed and occurred as the nanocrystal began to transition away from the monoclinic structure. This was followed by a slower reduction in the Bragg angle. We understand this to result from the step-wise motion of atoms in the unit cell during the transition. The rotation of the V-V pairs can be considered to occur in two stages. First a faster expansion of the vanadium pair and finally a slower shearing of the pair. This is in agreement with previous studies performed using electron diffraction on bulk samples. [26] From the figure 2 we obtain a maximum speed of more than 0.007 m/s for the expansion of the (011) lattice planes. The (110) reflection of the high temperature tetragonal structure is predicted to have a Bragg angle of 0.99 mrad below that of the (011) reflection of the monoclinic (M_1) structure and is therefore ideal for observing both structures in tandem on a single detector plane. In order, however, to observe femto-second angular deviations, it is essential that diffraction is observed from a lattice plane with a significant component in the plane of the V-V atom pair rotation. This is equivalent to Miller indices (hkl)

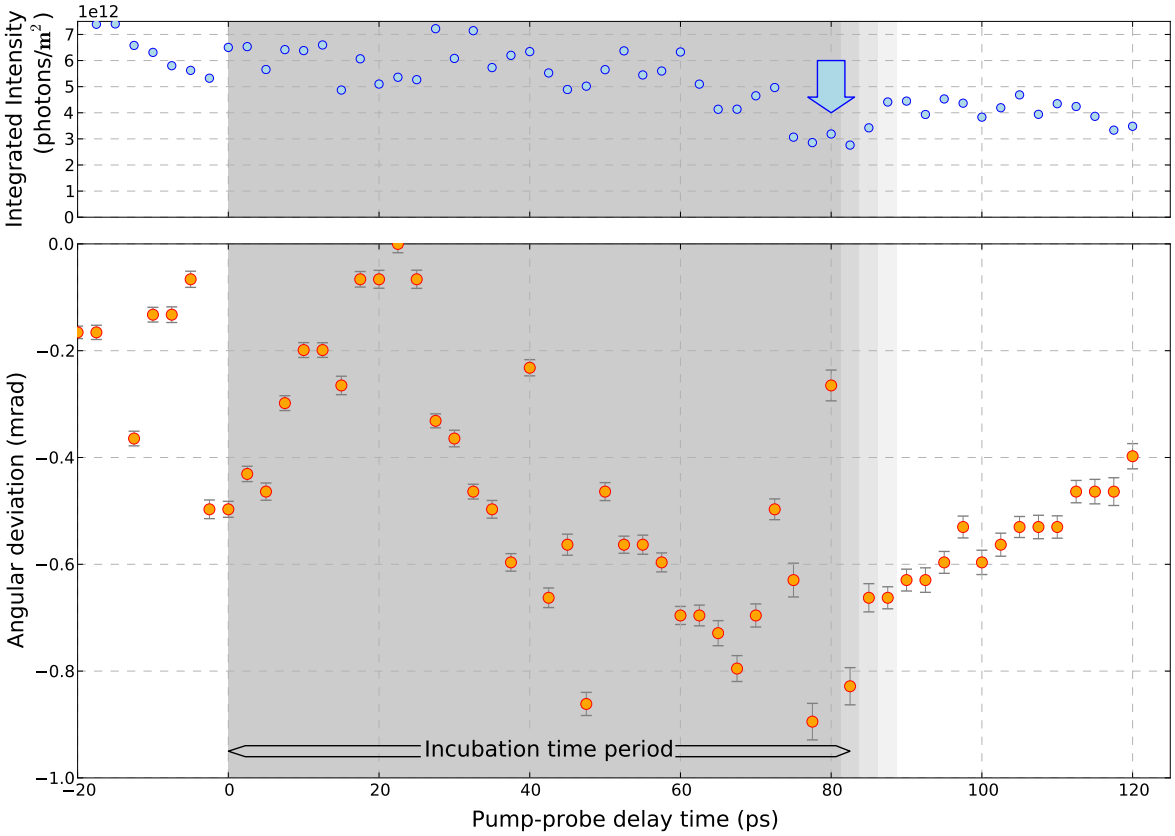

FIG. 3. **Angular deviation and integrated intensity of the coherent diffraction pattern at increased excitation**. Initial stages of the deviation of the displacement of the maximum intensity in response to excitation at a fluence of 306 mJ/cm^2 per pulse from the Ti:Sapphire femto-second laser excitation source. The integrated intensity is also shown and reduces by $\sim 4 \times 10^{12}$ photons/m^2 during the structural phase transition, as indicated. Each data point results from the accumulation of data from 25 XFEL shots with dark-field subtraction.

for which h and l are non-zero. Angular deviation of diffraction from the (011) reflection therefore occurs on the pico-second time scale as we have a significant out of plane component of the transfer wavevector **Q**. Oscillations in the angular deviation are also apparent and were best fitted to a damped harmonic oscillator equation with frequencies at 8.1 GHz, 55.8 GHz and 26.5 GHz (see Supplementary Information). Coherent phonons propagating within the nanocrystal are the likely cause where the oscillation frequencies are strongly coupled to the geometry of the nanocrystal. Figures 2**b** and 2**c** show the coherent diffraction patterns at delay times of 0 ps and 62.5 ps respectively. Elongation of the coherent diffraction pattern occurs after 0 ps delay rather than a simple shift to lower angle. This is a result of strain in the nanocrystal arising due to competing intermediate monoclinic (M_2) and triclinic phases as the lattice planes expand.[8, 27, 28]

Figure 3 shows the angular deviation of the coherent diffraction pattern for varying delay times at an increased excitation of 306 mJ/cm^2 per pulse from the Ti:Sapphire femto-second laser excitation source. Each data point results from the accumulation of data from 25 XFEL shots with dark-field subtraction. At this excitation energy, we were able to observe a structural transition. We found that during an incubation period of 92.5 ps, the intensity peak of the coherent diffraction pattern moved between various locations within the diffraction pattern. This is likely due to internal strain and plastic deformation of the nanocrystal. During the incubation period, the mean displacement of the Bragg angle did not return to zero after each excitation cycle suggesting that the crystal had not completely returned to its original structure (see supplementary information). This is likely due to the crystal becoming trapped in an intermediate monoclinic phase with a Bragg angle between that of the monoclinic M_1 and tetragonal phases. After an incubation period of 92.5 ps the original coherent diffraction pattern was no longer visible and a coherent new diffraction pattern emerged. Toward the end of this period and at a delay of 80 ps, the integrated intensity reduced by $\sim 4 \times 10^{12}$ photons/m^2 (as indicated in figure 3) for 12.5 ps, after which the coherent diffraction

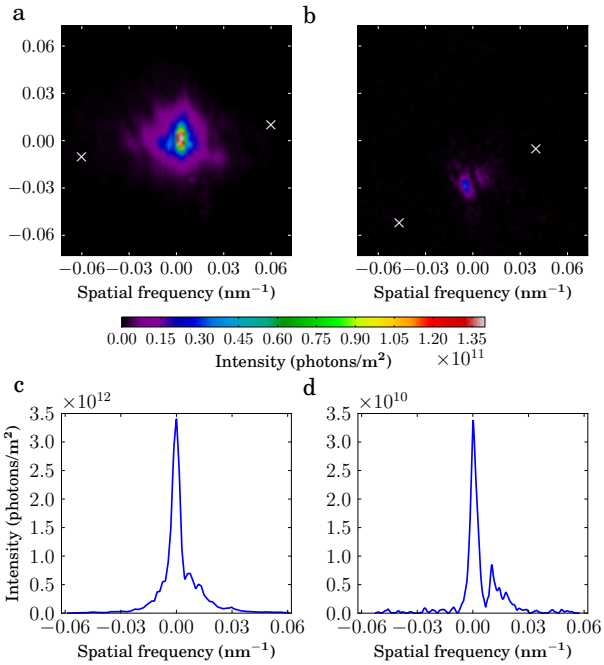

FIG. 4. **Coherent diffraction pattern of monoclinic and tetragonal structures**. Coherent diffraction patterns in response to excitation at a fluence of 306 mJ/cm^2 per pulse from the Ti:Sapphire femto-second laser at **a**, 0 ps delay and **b**, 92.5 ps delay. Intensity line scans through the points marked "×" are shown in **c** and **d**, respectively.

pattern of the new phase emerged.

Figure 4**a** and figure 4**b** shows the coherent diffraction pattern correspondig to figure 3 at time delays of 0 ps and 92.5 ps respectively. The displacement of the centre of the Bragg peak of the new coherent diffraction pattern was at most 0.89 mrad below the original agreeing reasonably well with theoretical predictions. We take into consideration that the diffractometer remained in the Bragg geometry for the monoclinic phase during measurements and therefore only partially satisfied that of the tetragonal phase. It is therefore likely that the observed diffraction is from the high temperature tetragonal phase. Line scans drawn between points marked "×" in figure 4**a** and figure 4**b** are shown in figure 4**c** and 4**d**, respectively. Comparable fringe spacings of 0.0046 and 0.0052 nm^{-1} are obtained for the monoclinic and tetragonal phase respectively.

In summary, we have performed time resolved coherent X-ray diffraction measurements on a single nanoscale crystal of vanadium dioxide. We have observed ultra-fast dynamics of the phase transition from monoclinic to tetragonal structure. Step-wise motion of atoms in the unit cell was observed during the transition and attributed to rotation of the V-V pairs. This study also demonstrates the feasibility of the XFEL for the study of structural changes in correlated electronic materials. With further improvements to iterative phase retrieval algorithms for reconstructing strained crystalline structures, it should also be possible to invert coherent diffraction patterns from time-resolved measurements to obtain real-space images. This ultimately will provide a means to obtain real-space time-lapse images of the object with femto-second resolution.

METHODS

Self-assembled VO_2 nanocrystals were synthesised in bulk quantity using a high temperature chemical vapour transport and deposition (CVTD) process at 900°C and at a pressure of 10 Pascals. A single VO_2 nanocrystal was then transferred to a clean Si (100) substrate, scored into four quadrants. Temperature dependent micro-Raman measurements were then performed on a single VO_2 nanocrystals to confirm the transition temperature. Subsequently, a single vanadium dioxide crystal was selected and prepared on a Silicon substrate as shown in figure 1.

The following procedure was used to determine an appropriate initial sample temperature for pump-probe measurements. The sample was heated to 30°C. A coherent diffraction pattern from the low temperature monoclinic (011) reflection was then recorded. The sample was subsequently heated through the transition into the high temperature tetragonal phase at which point the diffraction intensity disappeared. The temperature at which this occurred was recorded. The Bragg angle and sample orientation were then changed to locate the (110) reflection of the high temperature Rutile phase and a coherent diffraction pattern was recorded. After this, the Bragg angle and sample orientation was returned to that of the low temperature (011) monoclinic reflection and the sample cooled until this coherent diffraction pattern was again visible. This process was found to be stable if the sample was return to 30°C. A temperature of 30°C was therefore maintained throughout the experiment.

ACKNOWLEDGEMENTS

We would like to thank the operations staff scientists at SACLA for the performance and flexibility of the XFEL throughout our experiments. We would also like to thank the software engineers for their efforts in producing a capable data acquisition system with analysis capabilities.

This work was funded by the Japan Society for the Promotion of Science (JSPS) Young Researcher Kakenhi award, grant number 24681014.

AUTHOR CONTRIBUTIONS

M.C.N., Y.N. and Y.T. planned the experiments. VO_2 nanocrystals were prepared by M.C.N. Experimental data was gathered by all authors. Data analysis was carried out by M.C.N. The manuscript was prepared by M.C.N.

* M.Newton@es.hokudai.ac.jp

[1] Y. Tokura, Physics Today **56**, 50 (2003).

[2] A. Tselev, J. D. Budai, E. Strelcov, J. Z. Tischler, A. Kolmakov, and S. V. Kalinin, Nano Letters **11**, 3065 (2011).

[3] M. Fiebig, K. Miyano, Y. Tomioka, and Y. Tokura, Science **280**, 1925 (1998).

[4] B. Kundys, M. Viret, D. Colson, and D. O. Kundys, Nat Mater **9**, 803 (2010).

[5] G. Kotliar and D. Vollhardt, Physics Today **57**, 53 (2004).

[6] H. S. Park, O.-H. Kwon, J. S. Baskin, B. Barwick, and A. H. Zewail, Nano Letters **9**, 3954 (2009), pMID: 19856902.

[7] R. M. Wentzcovitch, W. W. Schulz, and P. B. Allen, Phys. Rev. Lett. **72**, 3389 (1994).

[8] A. Zylbersztejn and N. F. Mott, Phys. Rev. B **11**, 4383 (1975).

[9] A. Cavalleri, T. Dekorsy, H. H. W. Chong, J. C. Kieffer, and R. W. Schoenlein, Phys. Rev. B **70**, 161102 (2004).

[10] H.-T. Kim, Y. W. Lee, B.-J. Kim, B.-G. Chae, S. J. Yun, K.-Y. Kang, K.-J. Han, K.-J. Yee, and Y.-S. Lim, Phys. Rev. Lett. **97**, 266401 (2006).

[11] G. Stefanovich, A. Pergament, and D. Stefanovich, Journal of Physics: Condensed Matter **12**, 8837 (2000).

[12] Y. W. Lee, B.-J. Kim, J.-W. Lim, S. J. Yun, S. Choi, B.-G. Chae, G. Kim, and H.-T. Kim, Applied Physics Letters **92**, 162903 (2008).

[13] T. Driscoll, H.-T. Kim, B.-G. Chae, M. D. Ventra, and D. N. Basov, Applied Physics Letters **95**, 043503 (2009).

[14] C. Zhou, D. M. Newns, J. A. Misewich, and P. C. Pattnaik, Applied Physics Letters **70**, 598 (1997).

[15] G. Margaritondo and P. R. Ribic, Journal of Synchrotron Radiation **18**, 101 (2011).

[16] M. M. Seibert, T. Ekeberg, F. R. N. C. Maia, M. Svenda, J. Andreasson, O. Joensson, D. Odic, B. Iwan, A. Rocker, D. Westphal, M. Hantke, D. P. DePonte, A. Barty, J. Schulz, L. Gumprecht, N. Coppola, A. Aquila, M. Liang, T. A. White, A. Martin, C. Caleman, S. Stern, C. Abergel, V. Seltzer, J.-M. Claverie, C. Bostedt, J. D. Bozek, S. Boutet, A. A. Miahnahri, M. Messerschmidt, J. Krzywinski, G. Williams, K. O. Hodgson, M. J. Bogan, C. Y. Hampton, R. G. Sierra, D. Starodub, I. Andersson, S. Bajt, M. Barthelmess, J. C. H. Spence, P. Fromme, U. Weierstall, R. Kirian, M. Hunter, R. B. Doak, S. Marchesini, S. P. Hau-Riege, M. Frank, R. L. Shoeman, L. Lomb, S. W. Epp, R. Hartmann, D. Rolles, A. Rudenko, C. Schmidt, L. Foucar, N. Kimmel, P. Holl, B. Rudek, B. Erk, A. Hoemke, C. Reich, D. Pietschner, G. Weidenspointner, L. Strueder, G. Hauser, H. Gorke, J. Ullrich, I. Schlichting, S. Herrmann, G. Schaller, F. Schopper, H. Soltau, K.-U. Kuehnel, R. Andritschke, C.-D. Schroeter, F. Krasniqi, M. Bott, S. Schorb, D. Rupp, M. Adolph, T. Gorkhover, H. Hirsemann, G. Potdevin, H. Graafsma, B. Nilsson, H. N. Chapman, and J. Hajdu, Nature **470**, 78 (2011).

[17] H. N. Chapman, P. Fromme, A. Barty, T. A. White, R. A. Kirian, A. Aquila, M. S. Hunter, J. Schulz, D. P. DePonte, U. Weierstall, R. B. Doak, F. R. N. C. Maia, A. V. Martin, I. Schlichting, L. Lomb, N. Coppola, R. L. Shoeman, S. W. Epp, R. Hartmann, D. Rolles, A. Rudenko, L. Foucar, N. Kimmel, G. Weidenspointner, P. Holl, M. Liang, M. Barthelmess, C. Caleman, S. Boutet, M. J. Bogan, J. Krzywinski, C. Bostedt, S. Bajt, L. Gumprecht, B. Rudek, B. Erk, C. Schmidt, A. Hoemke, C. Reich, D. Pietschner, L. Strueder, G. Hauser, H. Gorke, J. Ullrich, S. Herrmann, G. Schaller, F. Schopper, H. Soltau, K.-U. Kuehnel, M. Messerschmidt, J. D. Bozek, S. P. Hau-Riege, M. Frank, C. Y. Hampton, R. G. Sierra, D. Starodub, G. J. Williams, J. Hajdu, N. Timneanu, M. M. Seibert, J. Andreasson, A. Rocker, O. Joensson, M. Svenda, S. Stern, K. Nass, R. Andritschke, C.-D. Schroeter, F. Krasniqi, M. Bott, K. E. Schmidt, X. Wang, I. Grotjohann, J. M. Holton, T. R. M. Barends, R. Neutze, S. Marchesini, R. Fromme, S. Schorb, D. Rupp, M. Adolph, T. Gorkhover, I. Andersson, H. Hirsemann, G. Potdevin, H. Graafsma, B. Nilsson, and J. C. H. Spence, Nature **470**, 73 (2011).

[18] J. N. Clark, L. Beitra, G. Xiong, A. Higginbotham, D. M. Fritz, H. T. Lemke, D. Zhu, M. Chollet, G. J. Williams, M. Messerschmidt, B. Abbey, R. J. Harder, A. M. Korsunsky, J. S. Wark, and I. K. Robinson, Science **341**, 56 (2013).

[19] J. Miao, P. Charalambous, J. Kirz, and D. Sayre, NATURE **400**, 342 (1999).

[20] I. Robinson and J. Miao, MRS Bulletin **29**, 177 (2004).

[21] M. Pfeifer, G. Williams, I. Vartanyants, R. Harder, and I. Robinson, Nature **442**, 63 (2006).

[22] D. Sayre, Acta Crystallographica **5**, 843 (1952).

[23] M. C. Newton, S. J. Leake, R. Harder, and I. K. Robinson, Nature Materials **9**, 120 (2010).

[24] T. Ishikawa, H. Aoyagi, T. Asaka, Y. Asano, N. Azumi, T. Bizen, H. Ego, K. Fukami, T. Fukui, Y. Furukawa, S. Goto, H. Hanaki, T. Hara, T. Hasegawa, T. Hatsui, A. Higashiya, T. Hirono, N. Hosoda, M. Ishii, T. Inagaki, Y. Inubushi, T. Itoga, Y. Joti, M. Kago, T. Kameshima, H. Kimura, Y. Kirihara, A. Kiyomichi, T. Kobayashi, C. Kondo, T. Kudo, H. Maesaka, X. M. Marechal, T. Masuda, S. Matsubara, T. Matsumoto, T. Matsushita, S. Matsui, M. Nagasono, N. Nariyama, H. Ohashi, T. Ohata, T. Ohshima, S. Ono, Y. Otake, C. Saji, T. Sakurai, T. Sato, K. Sawada, T. Seike, K. Shirasawa, T. Sugimoto, S. Suzuki, S. Takahashi, H. Takebe, K. Takeshita, K. Tamasaku, H. Tanaka, R. Tanaka, T. Tanaka, T. Togashi, K. Togawa, A. Tokuhisa, H. Tomizawa, K. Tono, S. Wu, M. Yabashi, M. Yamaga, A. Yamashita, K. Yanagida, C. Zhang, T. Shintake, H. Kitamura, and N. Kumagai, Nat Photon

advance online publication (2012), 10.1038/nphoton.2012.141.

[25] Y. Inubushi, K. Tono, T. Togashi, T. Sato, T. Hatsui, T. Kameshima, K. Togawa, T. Hara, T. Tanaka, H. Tanaka, T. Ishikawa, and M. Yabashi, Phys. Rev. Lett. **109**, 144801 (2012).

[26] P. Baum, D.-S. Yang, and A. H. Zewail, Science **318**, 788 (2007).

[27] T. M. Rice, H. Launois, and J. P. Pouget, Phys. Rev. Lett. **73**, 3042 (1994).

[28] A. Tselev, I. A. Luk'yanchuk, I. N. Ivanov, J. D. Budai, J. Z. Tischler, E. Strelcov, A. Kolmakov, and S. V. Kalinin, Nano Letters **10**, 4409 (2010).